



## TWO DIMENSIONAL STRESS ANALYSIS OF STRUCTURAL MEMBERS WITH CENTRAL HOLES AND EDGE NOTCHES

Riyadh J. Aziz, Adel A. Al-Azzawi and Hussam K. Risan

Department of Civil Engineering, Nahrain University, Baghdad, Iraq

E-Mails: [riyadhaziz48@yahoo.com](mailto:riyadhaziz48@yahoo.com)

### ABSTRACT

Analytical solutions for structures with opening were only derived for limited domains with very simple geometry. Although the finite element method (FEM) computes accurately the displacements, it is ineffective in determining the stresses in area of large stress gradients. The boundary element method (BEM) has been adopted in this paper which is well suited for solving problems in domains with geometric discontinuities. The stress concentration factors (S.C.F) for various holes and edge notches in structural members have been evaluated numerically based on the written BEM program and experimentally based on laboratory testing of representative specimens coupled with strain gauge techniques. Verification problems and real structural problems were investigated using both the present BEM program and FEM. A very coarse mesh was used in BEM while a very fine mesh was used in FEM. It has been shown that both BEM and FEM give closer results in term of displacement (not more than 2% difference) when changing the used element numbers in both methods. On the other hand, the stress field of both methods has a significant difference (more than 10%) and this difference becomes diverging in a region of a rapid stress variation. The experimental work includes testing seven steel plates specimens made from steel having thickness of 5.6mm; two specimens from each test are made for verification purposes. The specimens were made with different geometric discontinuities (central holes and edge notches with different sizes). A universal testing machine is used to apply a tensile force incrementally up to failure. A point-to-point experimental technique was used to measure the S.C.F by using a rectangular rosette strain gauge. Three specimens were analyzed numerically using BEM to examine the validity of the present study BEM program for solving such problems. It has been recorded experimentally that the S.C.F for the hole and notch specimens are not a function of load history. The stress concentration factor for the hole and notch specimens varies with the variation in the size and type of hole and notch.

**Keywords:** boundary element method, stress concentration factor, strain gauge technique, tension plate with hole and notch.

### INTRODUCTION

A reasonable question to ask is why there is a need to use the BEM since the FEM has already been used to solve engineering problems. The answer is that a modeling with finite elements can be ineffective and laborious for certain classes of problems. So the FEM, despite the generality of its application in engineering problems, is not free of drawbacks, the most important of which are:

The Discretization is over the entire domain occupied by the body. Hence, generation and inspection of the finite element mesh exhibit difficulty and are both laborious and time consuming; especially when there are holes, notches, mesh refinement and high element density are required at these critical regions.

Modification of the discretized model to improve the accuracy of the solution or to reflect design changes can be difficult and required a lot of effort and time.

Although the FEM computes accurately the field function, (displacement), which is the unknown of the problem, it is ineffective in determining its derivatives, (tractions or stresses). The accuracy considerably drops in areas of large stress gradients.

BEM possesses many advantages, the most important of which are: The discretization is only over the boundary of the body, which means the dimensionality of the problem is reduced by one order. This means that the numbers of unknowns are reduced dramatically, because unknowns occur only on the problem boundary. Thus, a

remodeling to reflect design changes becomes simple. The method is particularly effective in computing the derivatives of the field function (e.g., fluxes, strains, stresses, and moments). It can easily handle concentrated forces and moments, either inside the domain or on the boundary. It gives very more accurate results in terms of stresses in areas of a large gradient.

At its current stage of development, the BEM exhibits the following main disadvantages:

Application of the BEM requires the so-called fundamental solution. The method cannot be used for problems whose fundamental solution is either not known or cannot be determined.

The numerical implementation of the BEM results in systems of linear algebraic equations whose coefficient matrices are fully populated and non-symmetric [Katsikadelis J.T. (2002)].

### NUMERICAL METHODS BACKGROUND

The numerical methods of continuum mechanics can be classified into three approaches: finite difference (FDM), finite element (FEM) and boundary element (BEM) methods. The finite difference approach is the simplest of the three approaches and is relatively easy to program. Its main serious drawback in practical engineering problems is that it is not suitable for problems with irregular geometries. Furthermore, because it is difficult to vary the size of the difference cells in particular regions, it is not suitable for problems of rapidly changing



variables, such as stress concentration problems. The FEM is very suitable for practical engineering problems of complex geometries. To obtain good accuracy in regions of rapidly changing variables, a large number of fine elements must be used. In the BEM approach, the governing differential equations are transformed into integral identities which are applicable over the surface or boundary. These integrals are numerically integrated over the boundary which is divided into small boundary elements. As in the other numerical approaches, provided that the boundary conditions are satisfied, a system of linear algebraic equations emerges for which a unique solution can be obtained. The BEM can easily accommodate geometrically complex boundaries. Furthermore, since all the approximations are restricted to the surface, it can model regions with rapidly changing variables with better accuracy than the FEM [Friedel Hartmann (1989)].

### HISTORICAL DEVELOPMENT

The fast problem leading to stress concentration was solved in 1898 by Kirch; he solved a problem of infinite plate with small circular hole. The solution was possible because of the development of polar coordinates in addition to rectangular Cartesian coordinates, so the hole can be modeled. From the polar coordinates, it can be easy to identify or specify the boundary conditions on the boundaries of the hole.

It took fifteen years for Inglis C. E. (1913) to go and repeat the same Kirch work for an elliptical hole. The first BEM was known as boundary integral equation method (BIEM), which is used as a method for solving problems of mathematical physics, has its origin in the work of Green G. (1828). He formulated the integral representation of the solution for the Dirichlet and Neumann problems of the Laplace equation by introducing the so-called Green's function for these problems. Betti E. (1872) presented a general method for integrating the equations of elasticity and deriving their solution in integral form. Basically, this may be regarded as a direct extension of Green's approach to the Navier equations of elasticity. Somigilana used Betti's reciprocal theorem to derive the integral representation of the solution for the elasticity problem, including in its expression the body forces, the boundary displacements and tractions.

The fatherhood, however, of the Boundary Element Method could be attributed to Fredholm. At the beginning of the twentieth century, he was the first one to use singular boundary integral equations in order to find the unknown boundary quantities for problems of potential theory. In fact the method was employed as a mathematical tool to determine the necessary boundary conditions for a well-posed problem of mathematical physics, and not as a method to solve the engineering problem. This is quite reasonable, because it was, and still is, not possible to find the analytical solution of the derived singular integral equations.

Closed form solutions of integral equations were only derived for some domains with very simple boundary

geometry. Unfortunately, the work of Fredholm predated the computers, which could make his ideas practical. For this reason, the Boundary Integral Equation Method was neglected until the end of the fifties. Then, with the advent of computers, the method came back to the spotlight as an appealing numerical method for solving engineering problems. Numerical methods were developed for the solution of boundary integral equations and difficult physical problems of complex boundary geometry, which could not be solved by other methods, were solved for first time by BEM. The first works that laid the foundation of BEM as a computational technique appeared in the early sixties. Jaswon M. A. (1963) and Symm G. T. (1963) used Fredholm's equations to solve two-dimensional problems of potential theory. The merits of BIEM, which were listed in the previous section, attract researchers and motivated them to further develop the method. Rizzo F. J. (1967) and Cruse T. (1969) applied the method to two- and three-dimensional elasticity problems, respectively. Rizzo F. J. and Shippy D. (1970) extended the method to anisotropic elasticity.

All the aforementioned problems are governed by second order partial differential equations. Another group of problems is those described by the biharmonic equation. In this case, the integral representation of the solution is derived from the Rayleigh-Green identity (Bergman S. and Schiffer M. (1953), and the approach is applied to plate bending and plane elasticity, with the latter being formulated in terms of Airy's stress function. The formulation consists of two boundary integral equations, one for each of the unknown boundary quantities. The first one arises from the boundary character of the integral representation of the field equation, while the second is obtained from the integral representation either of the Laplacian of the field function or its derivative along the normal to the boundary. The second approach presented by Katsikadelis *et al.* (1977) became the prevailing one and was adopted later by Bezine G. (1978) and Stern M. (1979) to solve the plate bending problem. An extended and detailed presentation of the plate bending problems that have been analyzed by the BEM can be found in Beskos D. E. (1991). The method has been established by the name BEM (Boundary Element Method), which is attributed to the approach used to solve the boundary integral equations (i.e., discretization of the boundary into elements). In 1978 organized the first international conference on BEM, and since then conferences on BEM are organized yearly by the International Society for Boundary Elements (ISBE) and the International Association for Boundary Elements (IABEM) [Partidge P. W., Brebbia C. A. and Wrobel L. C. (1992)]. Furthermore, all conferences on computational mechanics devote sessions to the BEM. A detailed review of this enormous work would occupy a lot of space in this research and, of course, it is beyond its scope.

Katsikadelis J. T. and Sapountzakis E. J. (1985) presented a boundary element solution for the Saint-Venant torsion problem for composite cylindrical bars of arbitrary cross section.



Mitao Ohga *et al.* (1991) performed a structural analysis based on combined use of the boundary element and transfer matrix which is applied to static problems of plated structures. In this paper, a transfer matrix is evaluated by combining two transfer matrices for in-plane and plate bending problems, which are derived from the systems of equations based on the ordinary boundary element method for in-plane and bending problems, respectively.

Thamer Najjar (1992) performed elastic and elasto-plastic boundary element formulation of plane structures. Two different problems were taken to present the adopted methods. The first part of the work deals with the use of the direct boundary element formulation for solving Reissner's plate model. The second part deals with the application of the boundary element method to elasto-plastic analysis of two-dimensional problems. Quadratic isoparametric elements were adopted for the analysis of the problems.

Hayder Abbas (1995) applied boundary element method to three dimensional transient elasto dynamic. The accuracy of reliability of this method was demonstrated by solving two examples for a spherical cavity under sudden radial expansion and spherical cavity under a pressure wave. Results are compared with the available analytical and numerical solutions.

Federico Pinto and Carlos A. Prato (2006) presented a formulation of the indirect boundary element method based on the principle of virtual work for the dynamic analysis of frame structures buried in semi-infinite elastic media.

Sapountzakis E. J. and Mokos V. G. (2011) developed a boundary element method for the non-uniform torsion of composite bar of arbitrary constant cross section. The composite bar consists of a matrix surrounding a finite number of inclusions.

## BEM FORMULATIONS

To arrive at a differential equation with displacements as the variables, three relationships have to be used: Equilibrium of a differential element (differential equations of stress), Hooke's law (stress-strain equations) and Strain definitions (strain-displacement equations). The above equation can be used and substituting in each other to get the displacement differential equation which is called the Navier equations which is written in tensor notation as:

$$\frac{\partial^2 u_i}{\partial x_j \partial x_j} + \left( \frac{1}{1-2\nu} \right) \frac{\partial^2 u_j}{\partial x_i \partial x_j} = \frac{-f_i}{G_s} \quad (1)$$

where  $f_i$  is the body forces and  $G_s$  is the shear modulus. The above equations can be solved by a complementary function and a particular integral. Therefore, the "fundamental solution" to Navier equations is sought. Navier equations can be transformed into biharmonic differential equations, for which solutions exist, by the following substitution:

$$u_i = \frac{\partial^2 G_i}{\partial x_j \partial x_j} - \frac{1}{2(1-\nu)} \frac{\partial^2 G_j}{\partial x_i \partial x_j} \quad (2)$$

The vector  $G$  is called the Galerkin vector, and the following biharmonic equations are obtained (Becker A. A., 1992):

$$\begin{aligned} \nabla^4 G_x &= \nabla^2 (\nabla^2 G_x) = \frac{-f_x}{G_s} \\ \nabla^4 G_y &= \nabla^2 (\nabla^2 G_y) = \frac{-f_y}{G_s} \end{aligned} \quad (3)$$

where  $\nabla^2$  is the Laplacian operator.

Consider the solution domain of Figure-1 with the load point  $p$  of coordinates  $(X_p)$  and  $(Y_p)$  and a field point  $Q$  on the boundary of coordinates  $(x_Q)$  and  $(y_Q)$ . Capital letters indicate fixed coordinates while lower case letters indicate variable coordinates. The fundamental solution is based on the three-dimensional classical solution of a point force in an infinite medium called the Kelvin solution. It can be easily verified that the following solutions satisfy the biharmonic equations (3) (Beer G. , 2008):

$$G_x = G_y = \frac{1}{8\pi G_s} r^2(p, Q) \ell n \left[ \frac{1}{r(p, Q)} \right] \quad (4)$$

where  $r(p, Q)$  is the distance between  $p$  and  $Q$  as:

$$r(p, Q) = \sqrt{(X_p - x_Q)^2 + (Y_p - y_Q)^2}$$

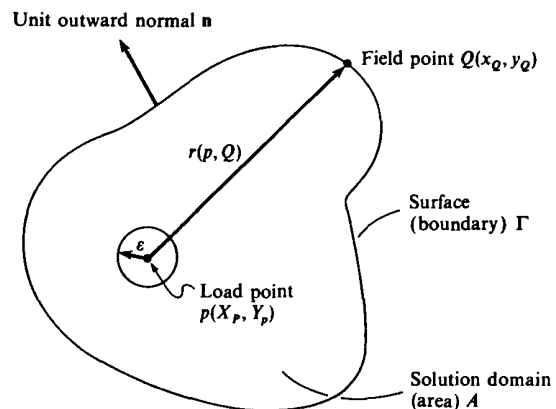


Figure-1. A two-dimensional physical domain (Becker A. A., 1992).

Substituting for  $G_x$  and  $G_y$  into Equations (2), the following expression for the displacement vector is obtained:

$$u_i = \frac{1}{8\pi G_s (1-\nu)} \left\{ (3-4\nu) \ell n \left[ \frac{1}{r(p, Q)} \right] \delta_{ij} + \frac{\partial r(p, Q)}{\partial x_i} \frac{\partial r(p, Q)}{\partial x_j} \right\} \quad (5)$$



The traction vector arising from the fundamental solution can be derived by differentiating the displacement vector and substituting in the Hooke's law equations as follows:

$$t_i = \frac{-1}{4\pi(1-\nu)r(p,Q)} \left( \frac{\partial r(p,Q)}{\partial n} \right) \left[ (1-2\nu)\delta_{ij} + 2 \frac{\partial r(p,Q)}{\partial x_i} \frac{\partial r(p,Q)}{\partial x_j} \right] + \frac{1-2\nu}{4\pi(1-\nu)r(p,Q)} \left[ \frac{\partial r(p,Q)}{\partial x_j} n_i - \frac{\partial r(p,Q)}{\partial x_i} n_j \right] \quad (6)$$

Betti's reciprocal work theorem and the Somigliana identity for the displacements can be used to derive an integral equation for the displacement at an interior point (p) due to tractions and displacements on the surface at a boundary point (Q). In the absence of body forces, this boundary integral equation (BIE) can be written as follows (Beer G. and Watson J. O., 1992):

$$u_i(p) + \int_{\Gamma} T_{ij}(p,Q)u_j(Q)d\Gamma(Q) = \int_{\Gamma} U_{ij}(p,Q)t_j(Q)d\Gamma(Q) \quad (7)$$

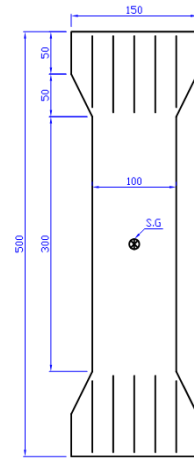
**BEM NUMERICAL IMPLEMENTATION**

The numerical implementation of elastostatic problems follows a very similar pattern to that of potential problems, and can be divided into six stages for convenience.

Stage One: Division of the Boundary into Elements, Stage Two: Numerical Integration of the kernels, Stage Three: Application of the Boundary Conditions, Stage Four: Solution of the Algebraic Equations, Stage Five: Calculation of the Boundary Stresses and finally, Stage Six: Calculation of the Internal Variables (Banerjee P. K.,1994).

**EXPERIMENTAL WORK**

Seven test specimens are made from steel plates having thickness of 5.6mm. For each type of test, two specimens were manufactured for verification purposes. The dimensions of the specimens, type of geometric discontinuities (i.e., holes and notches) and the location of the rosette strain gauge are shown in the Figures 2 to 4. The tested specimens are shown at the end of this paper. Each specimen is subjected to uniaxial tension until failure. The load increment, strain gauge reading was recorded at each load increment.



Control specimens (CS)

Figure-2. Control specimen (Units in mm).

Central $\Phi$ 25 Circular Hole ( $\Phi$ 25 CCH)	Central $\Phi$ 50 Circular Hole ( $\Phi$ 50 CCH)	Central 25x12.5 Hole (25x12.5 CH)	Central 50x25 Hole (50x25 CH)

Figure-3. Central hole specimens.

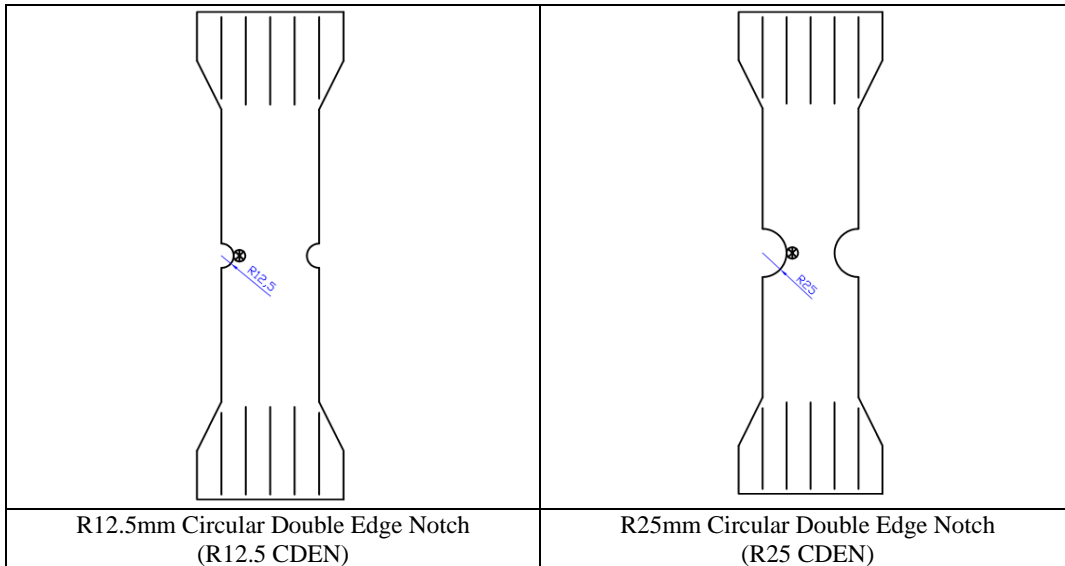


Figure-4. Circular double notches specimens.

Specimens were tested using universal testing machine Model: UBCH-001, manufactured by ALFA Co. Ltd. The load capacity of the machine is 2000 kN and it is equipped with computer panel for data printing and data transfer. The machine can also display the data and graphs on computer screen see Figure-5.



Figure-5. Universal tensile and compression tester model: UBCH-001.

The center point of the strain gauge is attached at distance 6 mm from the tip of holes and the three strain gauges in the rosette (1, 2 and 3) are aligned as  $\theta_1 = 135^\circ$ ,  $\theta_2 = 45^\circ$ ,  $\theta_3 = 90^\circ$  respectively as shown in Figure-6. Based on strain transformation equation, it is possible to obtain the components of strain tensor in Cartesian coordinates from these measurements as (Ramesh K., 2000):

$$\begin{aligned} \epsilon_1 &= \frac{1}{2}(\epsilon_{xx} + \epsilon_{yy} - \gamma_{xy}) \\ \epsilon_2 &= \frac{1}{2}(\epsilon_{xx} + \epsilon_{yy} + \gamma_{xy}) \\ \epsilon_3 &= \epsilon_{yy} \end{aligned} \tag{8}$$

Solving equations (8) for  $\epsilon_{xx}$ ,  $\epsilon_{yy}$  and  $\gamma_{xy}$  yields:

$$\begin{aligned} \epsilon_{xx} &= \epsilon_1 + \epsilon_2 - \epsilon_3 \\ \epsilon_{yy} &= \epsilon_3 \\ \gamma_{xy} &= \epsilon_2 - \epsilon_1 \end{aligned}$$

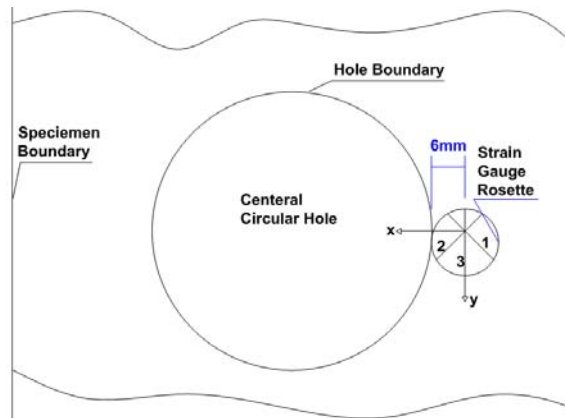


Figure-6. Location and alignment of the strain gauge rosette.

The measured state of surface strain and by assuming a plane stress situation, then the strain



components can be replaced by stress components by using the stress-strain relations. The actual pictures photos

of the current specimens are given in Figure-7 to 13:



**Figure-7. CS.**



**Figure-8.  $\phi$  25 CCH.**



**Figure-9.  $\phi$  50 CCH.**



**Figure-10. 25x12.5 CH.**



**Figure-11. 50x25 CH.**



**Figure-12. R12.5 CDEN.**



www.arpnjournals.com

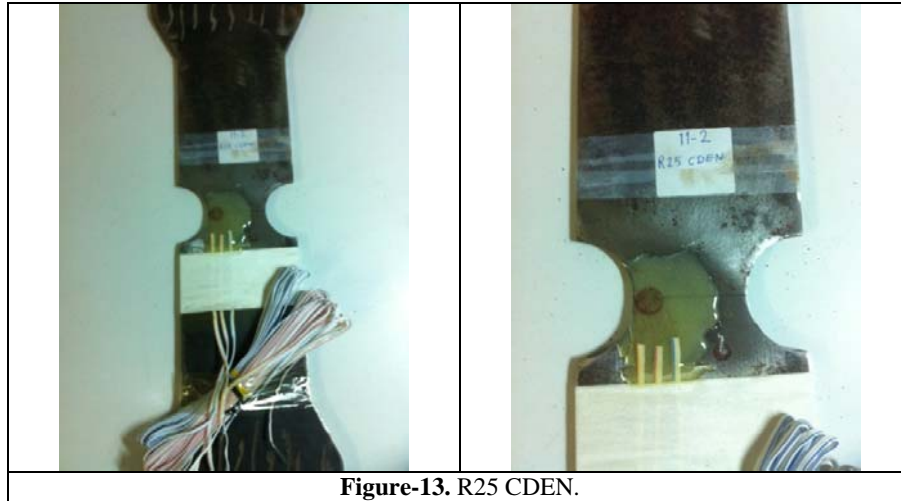


Figure-13. R25 CDEN.

### APPLICATIONS

A computer program based on BEM formulation and numerical implementation is developed and used to investigate practical two-dimensional problems to demonstrate the accuracy of the boundary element method for solving such problems. Special emphasis is placed on problems that exhibit a change in the geometry due to holes and notches of different sizes, shapes and locations.

#### Finite plate with a circular hole

Square plate of side length  $L$  containing a circular hole of radius ( $a$ ) and subjected to a uniaxial tensile stress  $\sigma_o$  is considered. The plate is assumed sufficiently thin for plane stress conditions to be valid. The numerical values used in this problem are  $L=2.0$ ,  $a=0.1$  and  $\sigma_o = 1.0$  with material properties  $E=1.0$  and  $\nu = 0.3$ . The analytical solution for the axial stress around a hole in an infinite plate is given by Timoshenko and Goodier (1970):

$$\frac{\sigma_{yy}}{\sigma_o} = 0.5 \left[ 2 + \left( \frac{a}{x} \right)^2 + 3 \left( \frac{a}{x} \right)^4 \right] \quad (10)$$

where  $x$  is a distance from the center of the hole. The BE mesh of 33 elements representing a quarter of the symmetrical geometry is shown in Figure-14. Node numbers are shown inside the domain, while element numbers are shown outside the domain (in circles).

The FE mesh discretizing a quarter of the symmetrical geometry are used and shown in Figure-15. Note that small size elements are placed in the region of expected rapid variation of stresses (around the hole) in both FE and BE methods. Figure-16 represents the numerical BE (33 elements, 66 nodes) stress concentration results around the hole in adjacent with the corresponding analytical and FE (226 elements, 745 nodes) solutions. The analytical solution slightly underestimates the stresses (not more than 2% relative to BEM) because of the assumption of an infinite plate. The BEM results are in good agreement with FEM with nil percentage difference in the results of the two methods even there is a large difference in the total degrees of freedom used in BEM formulation relative to FEM (degree of freedom used by BEM is 9% of that used by FEM).

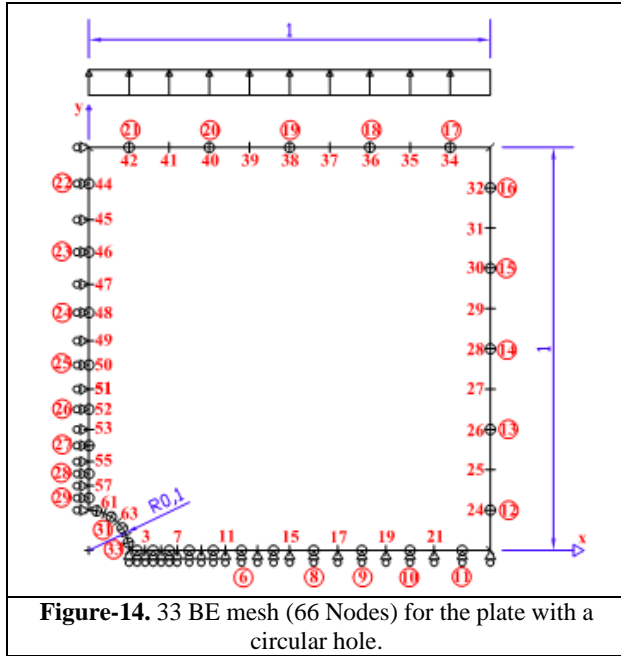


**Figure-14.** 33 BE mesh (66 Nodes) for the plate with a circular hole.

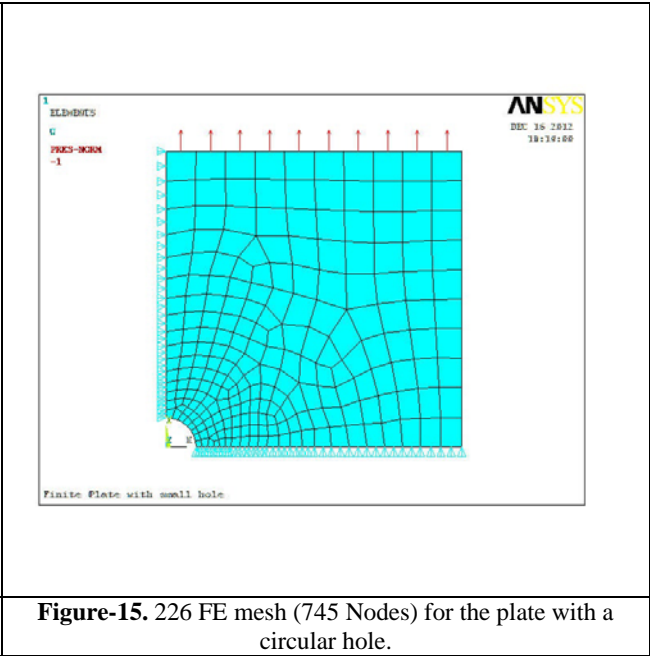


**Figure-15.** 226 FE mesh (745 Nodes) for the plate with a circular hole.

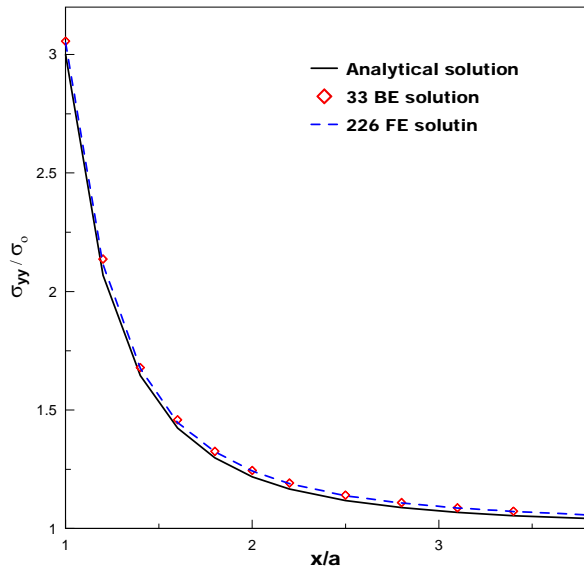


**Figure-16.** Stress concentration in the finite plate with a small circular hole.

axis of elliptical hole in an infinite plate is given by Inglis (1913).

$$\sigma_{\max} = \sigma_0(1 + 2a/b) \tag{10}$$

**Table-1.** Major and minor axes of ellipse.

(a)	(b)	(a/b)	$\sigma_{\max} / \sigma_0$
0.1000	0.10	1.0000	3.00
0.1000	0.05	2.0000	5.00
0.1250	0.04	3.1250	7.25
0.1667	0.03	5.5556	12.11
0.2500	0.02	12.5000	26.00

The BE mesh of 33 elements representing a quarter of the symmetrical geometry is shown in Figure-17. The parametric equation of the ellipse for constant angle increment is used to discretize the ellipse boundary into elements. Four elements discretization is used for each quarter (Hussam K. Risan, 2013).

**Finite plate with elliptical hole**

Square plate of side length L containing a central elliptical hole of major axis (2a) and minor axis of (2b) and subjected to uniaxial tensile stress  $\sigma_0$  is considered. The plate is assumed sufficiently thin for plane stress conditions to be valid. The numerical values used in this problem are L=2.0, a and b given in Table-1 below (to keep the area of the elliptical shape constant) and  $\sigma_0 = 1.0$  with material properties E=1.0 and  $\nu = 0.3$ . The analytical solution for the maximum axial stress at the tip of major

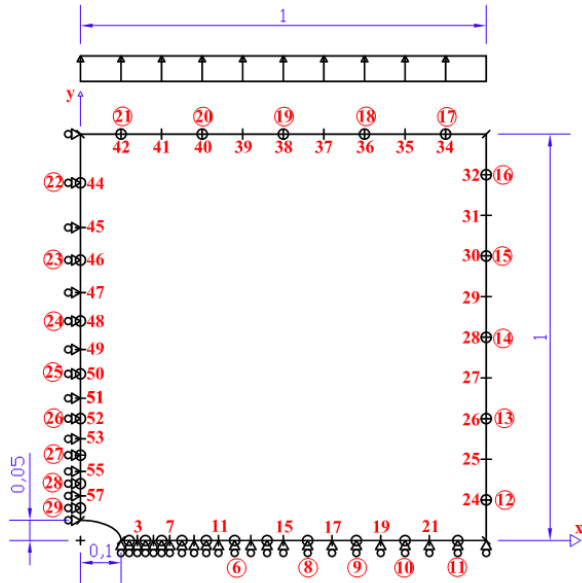


Figure-17. 33 BE mesh (66 Nodes) for the plate with elliptical hole.

The FE mesh discretizing a quarter of the symmetrical geometry with elliptical hole having  $a=0.1$  and  $b=0.05$  is used and shown in Figure-18. Note that small size elements are placed in the region of expected rapid variation of stresses (around the hole) in both FE and BE methods. Other elliptical hole sizes are discretized in the same manner with slightly different number of elements and nodes as illustrated in Table-2. For space purpose only elliptical hole has dimensions of  $a=0.1$  and  $b=0.05$  is shown.

The numerical maximum FE and BE stress concentration factor occurs at the tip of the major axis of the elliptical hole in adjacent with the corresponding analytical solutions for various  $a/b$  ratios are shown in Table-2 and Figure-19. The BE solution is more accurate relative to FE solution in comparison to analytical solution. When  $a/b$  ratio increases the FE solution diverges from the analytical values even a very large number of elements is used, while a reasonable result is obtained when using BEM with smaller number of boundary elements. The differences in ratios in terms of maximum stress concentration factors between the both numerical methods compared to analytical method is clearly shown in Table-2.

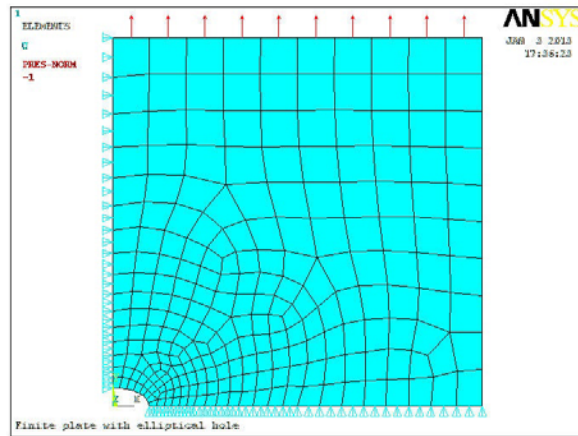


Figure-18. 236 FE mesh (775 Nodes) for the plate with an elliptical hole.

Table-2. BE and FE discretization and stress concentration factor for various  $a/b$ .

a/b	Analytical (A)	BEM (B)			FEM (F)		
		Mesh size	Factor	(A-B) / A *100 (%)	Mesh size	Factor	(A-F) / A *100 (%)
1.000	3.00	33 elements 66 nodes	3.0559	-1.86	226 elements, 745 nodes	3.0504	-1.68
2.000	5.00		4.6832	6.33	236 elements, 775 nodes	4.5630	8.74
3.125	7.25		7.1075	1.97	233 elements, 766 nodes	6.0700	16.28
5.556	12.11		11.289	6.78	210 elements, 697 nodes	8.6070	28.93
12.50	26.00		22.654	12.87	241 elements, 790 nodes	18.449	29.04

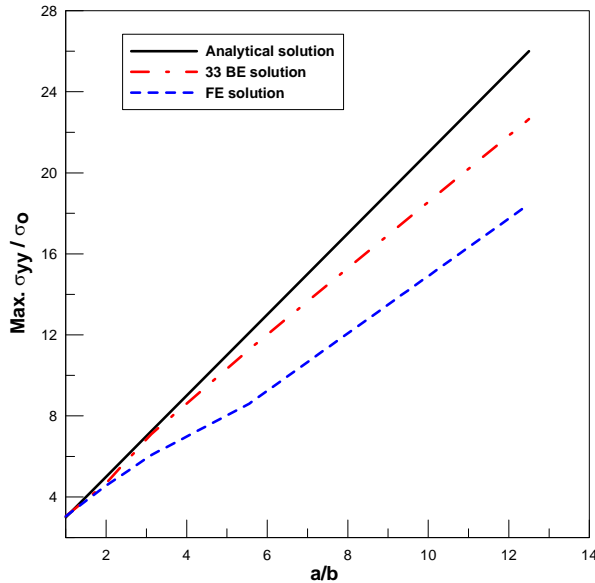


Figure-19. Maximum stress concentration factor for various a/b ratios for the plate with elliptical hole.

**Pipe under uniform internal pressure**

A rectangular pipe with dimensions and boundary conditions shown in Figure-20 subjected to internal pressure  $P=1MPa$  has been analyzed. It has a uniform cross-section and since it is very long in the z-direction, the produced state of stress is plane strain. The material constants are  $E=2 \times 10^5 kN/m^2$  and  $\nu=0.20$ . The BE mesh of 41 elements representing one-half of the symmetrical geometry is shown in Figure-21. The FE mesh discretizing one-half of the symmetrical geometry is used and shown in Figure-22. Note that small size elements are placed in the region of expected rapid variation of stresses (around the hole) in both FE and BE methods. The results are obtained using both the developed BEM program and FEM with ANSYS Software. In the BEM, the external boundary is divided into 41 boundary elements and the size of element far from rectangular hole is 0.25 while the size of the element around hole is 0.1.

Due to space considerations, the obtained results are given only at selected points. The distribution of y-displacement values in both BEM and FEM along  $y = 1.5m$  is shown in Figure-16 which reflects a good agreement in the displacement values in both methods in spite of using a few boundary numbers of elements in comparison the BEM with FEM. In the other hand, the distribution of traction  $t_y$  along the boundary  $y = 0$  is shown in Figure-17, whereas the distribution of  $\sigma_x$  along the boundaries  $y = 0$  and  $y=1.5m$  is shown in Figure-18 and Figure-19 respectively. Traction and stresses Figures show clearly the difference in the values of BEM compared with FEM in the region of high stress gradient.

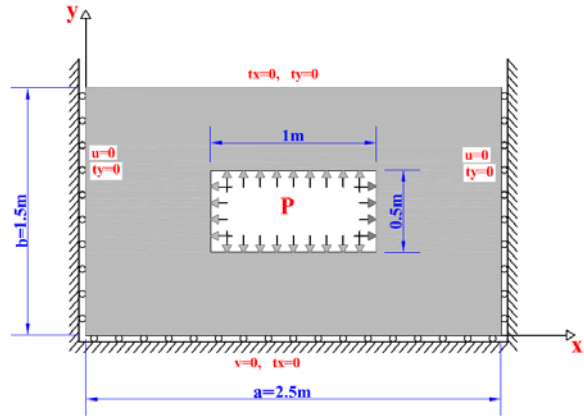


Figure-20. Pipe under uniform pressure (Plane strain).

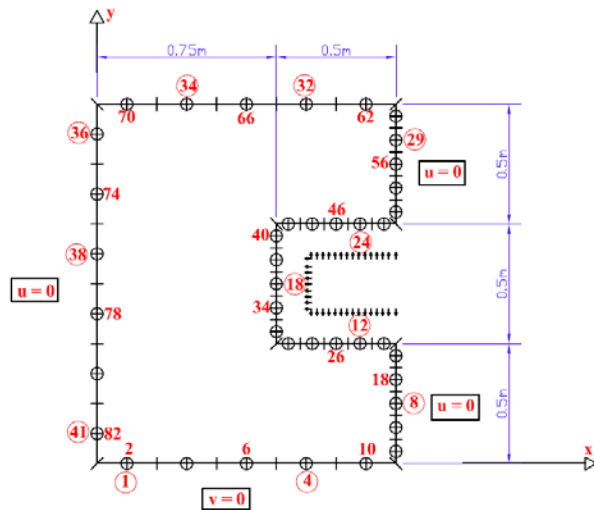


Figure-21. 41 BE mesh (82 Nodes) for the pipe with uniform pressure.

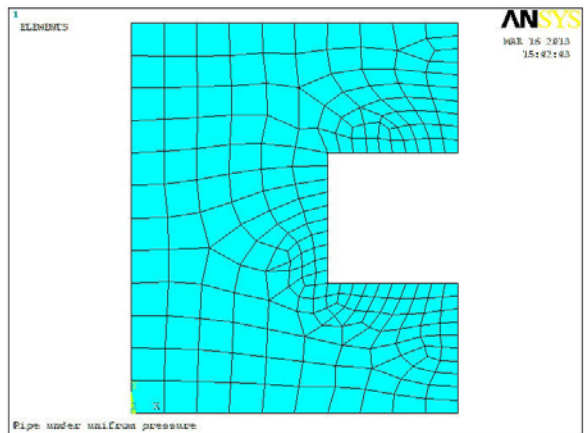
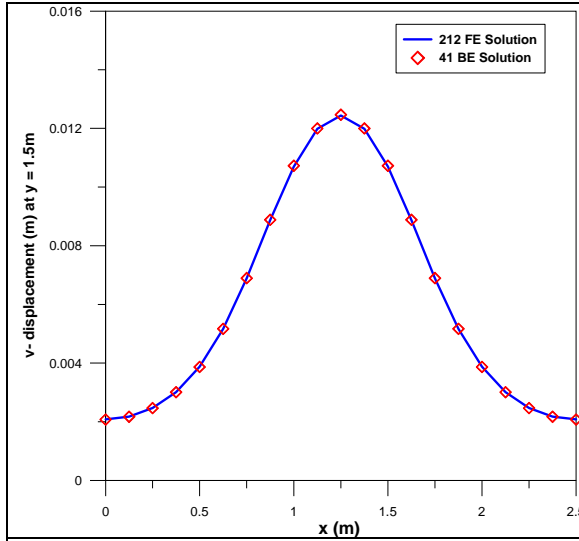
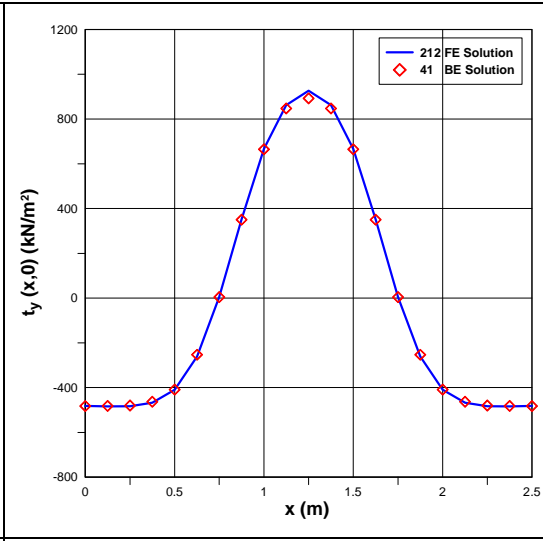


Figure-22. 212 FE mesh (717 Nodes) for the pipe with uniform pressure.



**Figure-23.** Distribution of y-displacement along the boundary  $y = 1.5$ .



**Figure-24.** Distribution of traction  $t_y$  along the boundary  $y = 0$ .

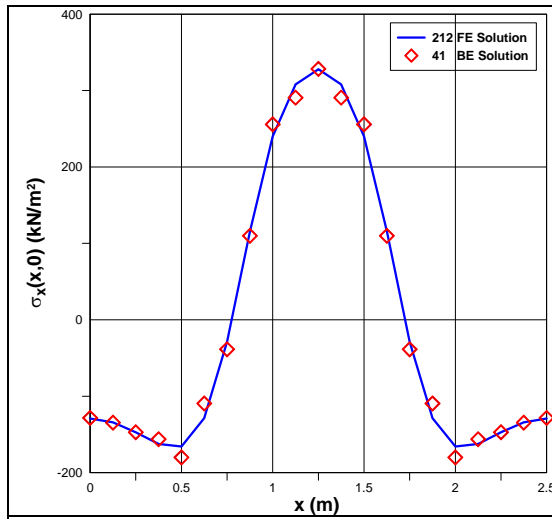


**Figure-25.** Distribution of  $\sigma_x$  along the boundary  $y = 0$ .

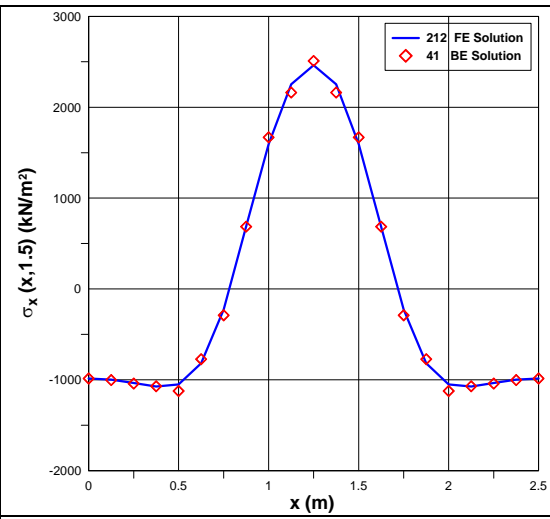


**Figure-26.** Distribution of  $\sigma_x$  along the boundary  $y = 1.5$ .

**EXPERIMENTAL RESULTS**

The laboratory results of the control specimens (CS), the material properties and geometry was found and illustrated in Table-3.

**Table-3.** CS Material properties and geometry.

Property/ Geometry	Measuring Value
Specimen thickness	5.6 mm
Specimen width	100 mm
Poisson ratio	0.28
Yield strength	251 MPa
Ultimate strength	332 MPa

Fracture strength	46 MPa
Modulus of elasticity	218 GPa

The ultimate strength of specimens with holes and notches that the specimens withstand before failure are given in Table-4. The ultimate strength varies with type and size of hole and notch. For each type of discontinuity, the ultimate strength decreases as the size of hole and notch increases. For the central hole (CCH and CH specimens), when the size of the hole is increased to 50%, a decrease in the ultimate strength of 29% is obtained. While a decrease of 33% in the ultimate strength occur when the size of notch increases to 50% in double notch specimen (CDEN specimens). The percentage decrease in the ultimate strength of the specimens



containing discontinuity (hole and notch) relative to the ultimate strength of the control specimen was calculated as shown in Table-4. The stress concentration factor for specimens with holes and notches were calculated using the measured strains. Three of these specimens namely  $\phi 50$  CCH, 50x25 CH and R25 CDEN had been solved

numerically using boundary element method. 50 elements (100 nodes) representing a quarter of the symmetrical geometry for each specimens was used in evaluation the stress concentration factor. The stress concentration factor (S.C.F) for the specimens that contain central holes and edge notches are illustrated in Table-5.

**Table-4.** Ultimate strength capacity of the specimens.

Specimen #	Specimen description	Specimen notation	(a) Ultimate stress (MPa)	$\frac{332-(a)}{332} * 100$ (%)
1	Control specimen	CS	332	0
2	Central $\phi 25$ mm Circular Hole	$\phi 25$ CCH	268	19.28
3	Central $\phi 50$ mm Circular Hole	$\phi 50$ CCH	188	43.37
4	Central 25x12.5 mm Hole	25x12.5 CH	254	23.50
5	Central 50x25 Hole	50x25 CH	179	46.08
6	R12.5mm Circular Double Edge Notch	R12.5 CDEN	284	14.46
7	R25mm Circular Double Edge Notch	R25 CDEN	191	42.47

**Table-5.** S.C.F for specimens with central holes and edge notches.

Specimen notation	(a) (MPa) applied average stress (P/A)	(b) (MPa) Stress from the strain gauge measurement	S.C.F Experimentally b/a	S.C.F BEM
$\phi 25$ CCH	25.00	46.28	1.85	-
	49.29	94.66	1.92	-
	74.04	143.42	1.94	-
$\phi 50$ CCH	25.63	39.00	1.98	2.00
	49.29	113.10	2.30	2.50
	74.32	174.65	2.35	2.55
25x12.5 CH	24.64	47.26	1.92	-
	49.02	95.28	1.94	-
	88.23	179.17	2.03	-
50x25 CH	28.8	83.25	2.89	2.90
	53.21	158.63	2.98	2.95
	73.84	232.41	3.14	3.20
R12.5 CDEN	24.11	36.41	1.51	-
	51.3	80.03	1.56	-
	75.36	122.10	1.62	-
R25 CDEN	25.38	40.20	1.60	1.70
	52.41	87.02	1.67	1.80
	72.89	127.20	1.74	1.85

In general, the specimens that contain central holes, high stress occurs in a section passing through the

center of the hole. While in notches, high stress will develop at the tip of the notch. Accordingly, the location



of the strain gauge was chosen at these locations. For specimens with discontinuities (with holes and notches) the state of stress near discontinuity is not uniaxial rather it's biaxial. For this reason, strain rosette is used to record the biaxial state of stress. From the data presented in Table-5 which concerns the study of the stress concentration factor for specimens that contain hole and notch. The following observations can be made:

Good agreement not less than approximately 90% is found between the experimental and numerical results in term of stress concentration factor for specimens containing hole and notch.

Using the BEM, the location of the failure plane is found to pass through the center of the hole or the

tip of the notch and these results are confirmed experimentally as shown in Figure 27 to 34 at the end of this paper.

It was found that the stress concentration factor for the hole and notch specimens does not vary with load history. Numerical and experimental results indicate that as the load increment increases, the stress concentration does not vary by more than 5%. The stress concentration factor for the hole and notch specimens varies with the variation in the size and type of hole and notch. When the size of the hole or the notch is decreased by 50%, the stress concentration factor is also reduced by approximately 20% for each type of hole and notch.



**Figure-27.** General setup.



**Figure-28.** Data logger.

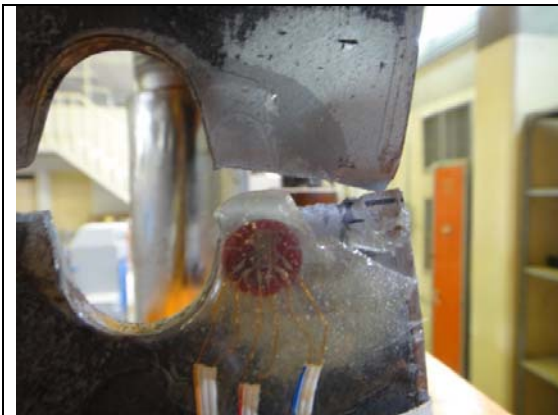


**Figure-29.**  $\phi$  25 CCH.



**Figure-30.**  $\phi$  50 CCH.



Figure-31. 25x12.5 CH.



Figure-32. 50x25 CH.



Figure-33. R12.5 CDEN.



Figure-34. R25 CDEN.

## CONCLUSIONS

Very good agreement is found between the experimental and numerical results based on boundary element method in term of stress concentration factor for specimens that contain hole and notch with maximum percentage difference of 10%.

- The stress concentration factor for the hole and notch specimens was found not varying with load history. Numerical use of boundary element method and experimental results indicate that as the load increment increases, the stress concentration factor does not vary by more than 5%.
- Experimentally and numerically using boundary element method has proved that the stress concentration factor for the hole and notch specimens varies with the variation in the size and type of hole and notch. When the size of the hole or the notch is decreased by 50%, the stress concentration factor is also reduced by approximately 20% for each type of hole and notch
- In the problem of finite plate with central circular hole, it can be concluded that even a small number of degrees of freedom is used to discretize the problem under consideration by BEM, a good result in term of stress field around the circular hole (or stress concentration factor) is reached in comparison with FEM results (the difference is not more than 1%). The total number of degrees of freedom used in BEM is (132) while the total number of degrees of freedom used in FEM is (1490) to reach approximately the same results.
- The analytical solution slightly underestimates the stress concentration factor around the circular hole compared with BEM results (the difference reaches to 2%) and this is because of the assumption of an infinite plate. It has been concluded that the stress concentration factor near the tip of the circular hole is about 3.06 using BEM while analytically it is 3.0.
- In the plate with elliptical hole with different a/b ratios, it has been shown that the BEM solution in term of stress field is more accurate than the FEM solution with respect to analytical solution. When a/b ratio increases, the FEM solution diverges from the analytical solution even when a very fine mesh is used (the difference relative to analytical solution reaches 30%), but still the BEM gives a reasonable results (not more than 12% difference). This is because when a/b ratio increases the problem under consideration must be tackled using the fracture mechanics instead of using only solid mechanics.



## REFERENCES

- Banerjee P. K. 1994. *The Boundary Element Methods in Engineering*. McGraw Hill International (UK) Limited.
- Beer G., Smith I. and Duenser C. 2008. *The Boundary Element Method with Programming*. Springer Wien New York.
- Beer G. and Watson J. O. 1992. *Introduction to Finite and Boundary Elements for Engineers*. J. Wiley.
- Becker A. A. 1992. *The Boundary Element Method in Engineering, A Complete Course*. McGraw-Hill International (UK) Limited.
- Bergman S. and Schiffer M. 1953. *Kernel Functions and Elliptic Differential Equations in Mathematical Physics*. Academic Press, New York.
- Bezine G. 1978. *Boundary Integral Equations for Plate Flexure with Arbitrary Boundary Conditions*. *Mechanics Research Communications*. 5:197-206.
- Beskos D. E. 1991. *Boundary Element Analysis of Plates and Shells*. Springer-Verlag, Berlin.
- Betti E. 1872. *Theory of Elasticity*. Cimento, Ser. 2: 7-10.
- Cruse T. 1969. *Numerical Solutions in Three-Dimensional Elastostatics*. *International Journal of Solids and Structures*. 5: 1259-1274.
- Friedel Hartmann 1989. *Introduction to Boundary Elements: Theory and Applications*. Springer-Verlag, Berlin.
- Federico P. and Carlos A. P. 2006. *Three-Dimensional Indirect Boundary Element Method Formulation for Dynamic Analysis of Frames Buried in Semiinfinite Elastic Media*. *Journal of Engineering Mechanics*. 132(9): 967-978.
- Green G. 1828. *An Essay on the Application on Mathematical Analysis to the Theory of Elasticity and Magnetism*. Nottingham.
- Hussam K. Risan. 2013. *Two-Dimensional Stress Analysis of structures with openings*, Ph.D thesis, Structural Eng. Al-Nahrain University.
- Hayder Majeed Abbas 1995. *On Boundary Element Method and Application for Three-Dimensional Transient Elasto-Dynamics*. M.Sc. thesis, Applied Mathematics, Al-Nahrain University.
- Inglis C. E. 1913. *Stresses in a Plate due to the Presence of Cracks and Sharp Corners*. *Transactions of the Institute of Naval Architects*. 55: 219-241.
- Jaswon M. A. 1963. *Integral Equation Methods in Potential Theory I*. *Proceedings of the Royal Society, Ser. A*. 275: 23-32.
- Katsikadelis J. T. 2002. *Boundary Elements, Theory and Application*. Elsevier, New York,.
- Katsikadelis J. T., Massalas C. V. and Tzivanidis G. J. 1977. *An Integral Equation Solution of the Plane Problem of the Theory of Elasticity*. *Mechanics Research Communications*. 4: 199-208.
- Katsikadelis J. T. and E. J. Sapountzakis E. J. 1985. *Torsion of Composite Bars by Boundary Element Method*. *Journal of Engineering Mechanics*. 111(9): 1197-1210.
- Mitao Ohga, Tsunemi Shigematsu and Taskashi Hara 1991. *Boundary Element-Transfer Matrix Method for Plated Structures*. *Journal of Engineering Mechanics*. 117(11): 2509-2526.
- Partidge P. W., Brebbia C. A. and Wrobel L. C. 1992. *The Dual Reciprocity Method*. Computational Mechanics Publications, Southampton.
- Ramesh K. 2000. *Experimental Stress Analysis*. Springer Verlag, Berlin.
- Rizzo F. J. 1967. *An Integral Equation Approach to Boundary Value Problems of Classical Elastostatics*. *Quarterly of Applied Mathematics*. 25: 83-95.
- Rizzo F. J. and Shippy D. 1970. *A Method for Stress Determination in Plane Anisotropic Elastic Bodies*. *Journal of Composite Materials*. 4: 36-61.
- Sapountzakis E. J. and Mokos V. G. 2011. *Non-uniform Torsion of Composite Bars by Boundary Element Method*. *Journal of Engineering Mechanics*. 127(9): 945-953.
- Symm G. T. 1963. *Integral Equation Methods in Potential Theory II*. *Proceedings of the Royal Society, Ser. A*. 275: 33-46.
- Stern M. 1979. *A General Boundary Integral Formulation for the Numerical Solution of Plate Bending Problems*. *International Journal of Solids and Structures*. 15: 769-782.
- Thamer Elia Yacoub Najjar 1992. *On the Elastic and Elasto-Plastic Boundary Element Formulation of Plane Structures*. M.Sc. Thesis, Civil Engineering Department, Al-Nahrain University.
- Timoshenko S. P. and Goodier J. N. 1970. *Theory of Elasticity*. Third edition, McGraw-Hill, Tokyo, Japan.